

C.R.N.

centre de recherches nucléaires de Strasbourg

CRN/PN 84-03

COHERENT PION PRODUCTION IN NUCLEI

Elle ASLANIDES
CENTRE DE RECHERCHES NUCLEAIRES
et
UNIVERSITE LOUIS PASTEUR
67037 STRASBOURG CEDEX, France

Institut National
de Physique Nucléaire
et de Physique
des Particules

Université
Louis Pasteur
de Strasbourg

COHERENT PION PRODUCTION IN NUCLEI

Elie ASLANIDES*

CENTRE DE RECHERCHES NUCLEAIRES et UNIVERSITE LOUIS PASTEUR

67037 STRASBOURG CEDEX, France

- * Invited talk given at the :
Colloque franco-japonais de confrontation des recherches nucléaires avec
des sondes électromagnétiques et hadroniques aux énergies intermédiaires.
Dogashima, 3-7 octobre 1983.

COHERENT PION PRODUCTION IN NUCLEI

Elie Aslanides
Centre de Recherches Nucléaires, 67037 Strasbourg Cedex, France
and
Université Louis Pasteur, Strasbourg France

Abstract : A survey of the recent proton induced π production experiments at Orsay and Saclay and a review of the recent heavier ion induced experiments at CERN, Orsay and Saclay are presented.

Since the pioneering experiments¹⁾ carried out at CERN and at Uppsala, a large number of studies of the coherent pion production by protons on nuclei, and its inverse reaction, have been carried out and a large theoretical effort has been devoted to this reaction. These efforts were motivated by the hope that this high momentum transfer reaction would become a new tool for studying high momentum components in nuclear wave functions, once its reaction mechanism is understood.

Incident proton energies from threshold and up to 800 MeV have been used on a variety of targets, ^3He to ^{90}Zr , and high quality data could be collected in many laboratories, UPPSALA, IUCF, TRIUMF, LAMPF. The experimental programs at ORSAY, SACLAY and at CERN made a large contribution to the high quality data near threshold and in the region of the 33 resonance.

The study of π -production in nuclei using heavier projectiles should help understanding the (p,π) production mechanism itself but also yield information on nuclear single particle momentum distributions, internal cluster momentum distributions and perhaps evidence for collective production, as a result of the coherent interaction of all or part of the target and projectile nucleons. These goals justify the experimental and theoretical efforts in the field without referring to more speculative and exciting ideas of shock waves in nuclear matter, phase transitions, pionic instability or fluctuations occurring at higher energies. The advent of intense heavier ion beams made possible to undertake π production experiments with deuterons (Saclay) and ^3He (CERN, Orsay, Saclay) at different energies and with ^{12}C ions of 86 MeV/nucleon at CERN.

THE (p,π) REACTION

Most of the experimental studies of the (p,π) reaction were undertaken below the free $\text{NN} \rightarrow \text{NN}\pi$ threshold of 292 MeV, where unlike the higher energy measurements, the data did show sensitivity to the nuclear structure. The angular distributions had in many cases "diffraction type" minima at momentum transfers which were energy independent and selectivity for high angular momentum states was noticeable.

The earlier work on (π^+,p) and (p,π^+) was carried out following single nucleon mechanism calculations (SNM)². However, given the high momentum transfers involved in pion production, $q \geq \sqrt{2mM} \sim 512$ MeV/c, it was reason-

able to extend the calculations to two or more active nucleons. Two-nucleon mechanisms, TNM³), are necessary for calculations of the (p, π^-) reaction, since the latter is certainly a two-nucleon process. Their most prominent difficulty will be to explain the suppression of the π^- relative to π^+ production. Among the recent developments we may notice the efforts to sum SNM and TNM coherently with a correct treatment of their interferences. At the present time, the question of the π production mechanism has no definite answer and it is not surprising that reaction mechanism and underlying nuclear structure cannot yet be distangled.

Recent studies of the (p, π) reaction at the Orsay synchrocyclotron include experiments on ^3He , ^4He , ^6Li , ^7Li and ^{10}B between 180 and 210 MeV^{4,5}). Angular distributions and the energy dependence have been measured, using targets of rather well known wave functions, in order to help understanding the production mechanism. Among all these results which are still being analyzed, the $p + ^3\text{He} \rightarrow \pi^+ + ^4\text{He}$ case⁶) is particularly interesting. A systematic analysis of (p, π) data over the whole range of the $s - p$ shell will be soon possible. Furthermore, the $p^3\text{He} \rightarrow \pi^+ ^4\text{He}$ reaction cross sections are used as an input to semi-phenomenological model calculations of the more complex three-nucleon transfer reaction ($^3\text{He}, \pi^+$).

Fig.1) shows the results of this experiment for three different energies. The angular distributions are structureless, but this is the case

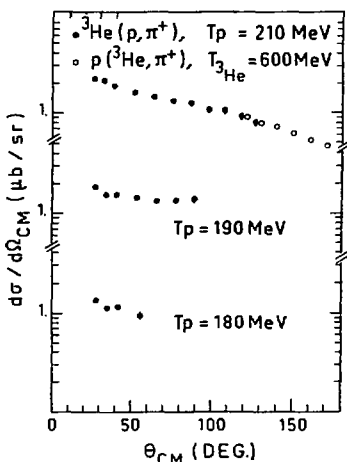


Fig.1. Differential cross sections of the $^3\text{He}(p, \pi^+)^4\text{He}$ reaction near threshold.

for many (p, π) reactions in the $1s - 1p$ shell. The cross sections are 100 times higher than in ^{90}Zr ⁶), indicating a strong target mass dependence. The results of the $^3\text{He}(p, \pi)$ experiment have been compared to those obtained from pionic atom data. The transition matrix elements derived from π -atomic shifts and widths⁷) are in good agreement with the results of the $^3\text{He}(p, \pi^+)$ experiment extrapolated to $k_\pi = 0$. The selectivity for specific nuclear states cannot be studied with this reaction. Measurements on heavier targets should be relevant to this question which remains controversial⁹⁻¹²).

The $^3\text{He}(p, \pi^+)$ data have been completed recently at Saturne⁸), in the study of the $^3\text{He} + p \rightarrow \pi^+ + ^4\text{He}$ reaction at forward pion angles, at $T_{^3\text{He}} = 600$ MeV, which correspond to $T_p = 200$ MeV and $120^\circ \leq \theta_{\pi}^{\text{LAB}} \leq 170^\circ$ for the $p + ^3\text{He} \rightarrow \pi^+ + ^4\text{He}$ reaction. The results of the Saturne experiment are shown by the open circles on fig.1), in excellent agreement with the lower energy data.

The data obtained far above threshold (Saclay, LAMPF, TRIUMF) investigated many different aspects of the (p, π) reaction. Very little similarities have been observed between low and high energy data and this is

understandable given the variation of the π -nucleus interaction below 600 MeV. The main features of the (p, π) reaction at higher energies can be summarized in the following points :

High spin states are preferentially excited in the final nuclei, as if a large angular momentum mismatch would be favoured by the high momentum transfers. Single particle and $2p$ - $1h$ states are equally excited.

The angular distributions of the emitted pions are structureless.

The comparison of π^+ and π^- production lead to the conclusion, that the leading reaction mechanism is different for the two reactions.

The (p, π^-) reaction is suppressed by a factor of $\sim 10^2$ compared to the (p, π^+) reaction.

The energy dependence of the two reactions is different. The (p, π^+) reaction cross sections increase from threshold to about 300 - 400 MeV before a decrease with energy up to 800 MeV. The (p, π^-) reaction cross section goes through a minimum around 600 MeV. The excitation functions are well described by a microscopic TNM involving a Δ (1232 MeV) intermediate excitation.

The (p, π^-) angular distributions vary with the incident energy.

The measurements of the analyzing power for the (p, π) reaction look promising in the investigation of its reaction mechanism. Dramatic changes of the analyzing power with the incident energy have been found¹³⁾. Many IUCF¹⁴⁾, TRIUMF¹³⁾ and LAMPF¹⁵⁾ data show that the nuclear structure modifies the analyzing power, so that one cannot consider the elementary reaction $pp \rightarrow \pi$ as the leading subprocess in the exclusive π production on nuclei.

Although no dedicated pion production experiments with protons have been carried out recently at Saclay, some experiments on meson production on very light targets are worth noticing. They have the merit of establishing relationships among many few-nucleon reactions and to contribute to the understanding of the meson production mechanism quite independently of its interplay with the nuclear structure.

The excitation function of the $pd \rightarrow \pi^+ p$ reaction at $\theta_\pi = 180^\circ$ has been measured¹⁶⁾ in the laboratory energy range $600 \leq T_p \leq 1500$ MeV using a liquid deuterium target and the SPES IV facility for the triton detection at forward angles. The striking similarity with the data of the backward elastic scattering of protons on ^3He is plausible in the framework of the OPE model¹⁷⁾ where all $B = 2$ exchange reactions are related to the backward pion deuteron scattering reaction as the "elementary" interaction. The OPE model with a double Δ propagation in the three nucleon system reproduces quite well the cross section enhancement around $T_p \approx 1.2$ GeV.

The $pd \rightarrow ^3\text{He} \pi^0$ reaction has also been studied in the energy range 925 to 1750 MeV for $140^\circ \leq \theta_\pi \leq 180^\circ$, using the SPES IV facility to detect the forward emitted ^3He particles¹⁸⁾. Fig.2) shows the preliminary results of the η^0 excitation function at $\theta_\eta = 180^\circ$ together with the results of the π^0 production at $\theta_\pi = 180^\circ$. The two excitation functions show a fast fall-off with energy before a maximum at ~ 1.35 GeV for η^0 and a second broader maximum for π^0 production around 1.2 GeV. The observed behaviour can be qualitatively attributed to N^* excitation in the intermediate state of the reaction and the ratio of the π^0 to the η^0 cross-sections related to the branching ratio of the N^* into the πN and $\eta^0 N$ channels.

The solid and dashed curves represent a OPE model calculation¹⁹⁾ in

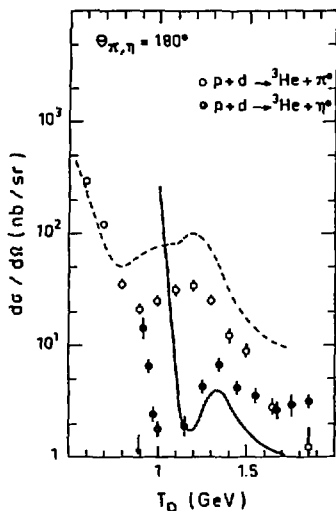


Fig.2. Excitation function of the $d(p, \pi^0)$ and $d(p, \eta^0)$ reactions at 180° .

The latter reaction is one of the most important inelastic channels of the NN interaction and as far as the subject of the present report is concerned, it has been introduced in DWIA calculations of the $pd + \pi^+$ reaction following the Ruderman prescription and in many theoretical calculations of the π production by protons and heavier ions. Alternatively, it is difficult to leave out of the list of arguments for studying this reaction the "hunting" of dibaryons. The results show a rapid change in shape for rather small energy steps, but the energy dependence of the coefficients describing the analyzing power, normalized to the total cross section appears to be smooth, except around 650 MeV where the Δ isobar intermediate state appears.

It is hoped that the availability of intense polarized beams of p and d at Saturne will stimulate further new experiments in the field of the pion production on nuclei.

PION PRODUCTION USING HEAVIER ION BEAMS

Inclusive pion production

Inclusive π production experiments are difficult to interpret and generally ambiguous since they are not complete, with regard to the final state identification. Pions in the continuum can be attributed to the elementary interaction $NN \rightarrow NN\pi$ of nucleons in the projectile and in the target and to a variety of coherent reactions involving substructures of several nucleons in the projectile or in the target. Recent progress in the theoretical calculation of nucleus-nucleus interactions make it possible to search for the manifestation of coherent π production, through the mea-

which it is assumed that the pion is emitted with the deuteron's momentum in the CM, leaving the deuteron at rest, and the backward nN partial waves have been parametrized in the multichannel formalism in order to introduce the different N^* with masses $1.52 \leq m_{N^*} \leq 1.9$ GeV. The calculation reproduces the π^0 to η^0 cross section ratio qualitatively and the overall shape and position of the observed structures. The discrepancy between the calculation and the experiment is subject to the neglect of off-shell effects as well as of initial and final state interactions. It seems that the coherent interaction of the three nucleons can give rise to an S-state type resonance which leads to a cross section enhancement in agreement with the experiment¹⁹).

The first pion production experiment which made use of the recently available polarized beam at Saturne, studied the analyzing power of the $\vec{p}p + d\pi^+$ reaction between 725 and 1000 MeV¹⁹) using the SPES I spectrometer.

surement of complete π spectra. Differences between the data and the theoretical calculations should be looked for, especially in the high energy side of the inclusive spectra where the validity of several models is better guaranteed. In the high-energy region, the probability of producing only one pion is large compared to the low-energy region. In that sense, the study of inclusive high energy π spectra can be complementary to the measurements of pion multiplicity distributions.

Rather complete inclusive pion production experiments could be carried out at the CERN Synchrocyclotron using the high intensity ${}^3\text{He}^{++}$ beam at 303 MeV/nucleon²¹⁾ and ${}^{12}\text{C}^{4+}$ beam at 86 MeV/nucleon²²⁻²⁴⁾. Some inclusive pion data could be measured using the deuteron beam²⁵⁾ of the Saturne synchrotron at Saclay at 300 MeV/nucleon.

The dependence of the cross sections on the target mass

The cross sections for low energy pion production, $T_{\pi} < 150$ MeV, at forward angles, using Ne beams at several energies between 80 and 535 MeV/nucleon²⁶⁾ are proportional to $\sqrt{A}^{2/3}$. The production of high energy pions, $P_{\pi} \geq 200$ MeV/c studied in the (${}^3\text{He}, \pi^-X$) experiments at 303 MeV/nucleon and at $\theta_{\pi} = 0^{\circ}$, followed a law $\sqrt{A}^{1/3}$ and the low exponent value of A indicated that high energy pions were produced in peripheral collisions²¹⁾. The low-energy pion production at larger angles using the ${}^{12}\text{C}$ beam at 86 MeV/nucleon²²⁾ follows a law \sqrt{A}^{α} with $0.5 < \alpha < 0.8$, indicating that these low energy pions were due predominantly to rather central collisions. However, in the forward angle (${}^{12}\text{C}, \pi^-X$) experiments²⁴⁾ the target mass dependence is very different. The invariant π^- cross sections for $P_{\pi} \geq 150$ MeV/c are proportional to $\sqrt{A}^{1.7 \pm 0.3}$, then saturate for $A \geq 27$ to $\sqrt{A}^{0.3 \pm 0.1}$. For the sake of completeness, we may notice that a recent experiment on high energy π production using the 183 MeV/nucleon Ne beam²⁷⁾ gave $A^{0.47}$ at 20°LAB and $\sqrt{A}^{0.83}$ at 90°LAB and that the observed angular dependence is consistent with an exponent $\alpha = 1/3$ at 0° . A different way to look at this rather complex A-dependence is to relate the integrated differential cross sections to the available CM energy $T_{CM} = \sqrt{s} - (M_{\text{proj.}} + M_{\text{target}})$ for the different targets (Fig. 3). The variation of the cross sections as a function of T_{CM} is almost linear and the extrapolation to zero cross section leads to a threshold energy of 302 ± 8 MeV.

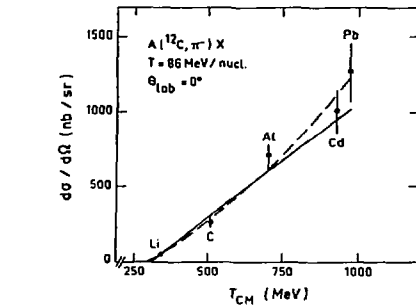


Fig.3. Integrated (${}^{12}\text{C}, \pi^-X$) reaction cross section as a function of the available CM energy.

The interpretation of such a behaviour would be that the pion production is due to a collective Δ excitation suggested theoretically by several authors²⁸⁻³⁰⁾. A calculation in the framework of the isobar model³⁰⁾ had successfully reproduced the shapes of the π spectra obtained with a 200 MeV/nucleon ${}^{20}\text{Ne}$ beam at 90°CM ²⁷⁾.

The comparison of π^- and π^+

The comparison of negative and positive pion production lead to many interesting observations. In the low energy π region the Berkeley experiment²⁶⁾ produced the first evidence of strong Coulomb effects and later the systematic study of these effects as a function of the incident energy³¹⁾. Strong Coulomb effects were observed through a large ratio $R_{\pi} = d\sigma(\pi^-)/d\sigma(\pi^+)$ for pions emitted at 0° , near the beam velocity and explained quantitatively in terms of Coulomb interactions between the pions and "cold" projectile fragments using Gyulassy's and Kaufmann's model³²⁾. Projectile fragments attract the π^- and repel the π^+ creating an enhancement of the R_{π} ratio along the beam direction.

Looking at the low energy pion data obtained with the ^{12}C beam at large angles²³⁾ (fig. 4) one observes a different behaviour of the π^- and π^+ production cross sections. In the

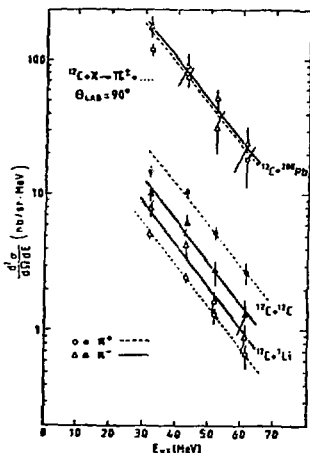


Fig. 4. π^+ and π^- differential cross sections of the $A(^{12}\text{C}, \pi X)$ reaction at 86 MeV/nucleon.

unity in apparent contradiction with the Berkeley Ne beam data²⁶⁾ which asymptotically decrease toward $R \approx 1$. Coulomb effects can be sensitive to details of the pion production model in a way which has yet to be established.

Differences between positive and negative pion production have also been observed for high energy pions in the $^{12}\text{C}(^3\text{He}, \pi^\pm X)$ reactions and attributed to nuclear structure effects. Large enhancements of the π^+ cross sections have been observed and attributed to the quasi free reaction $^3\text{He} + p \rightarrow \pi^+ + ^4\text{He}$ on s- and p-state protons in ^{12}C and to the $p + ^{12}\text{C} \rightarrow \pi^+ + ^{13}\text{C}$ reaction induced by individual s-state protons in ^3He ³³⁾.

Under adequate choice of projectile and target combinations, such measurements can develop into a method of determining internal momentum distributions of nucleons or clusters in nuclei.

The comparison to theoretical models

Many theoretical models have been proposed for the description of the nucleus-nucleus interactions and more specifically for the π production, between two rather extreme pictures : the single nucleon-nucleon model and the thermal model implying that the reaction takes place through a large number of nucleon-nucleon interactions, so that equilibrium is reached among all the participants in the reaction. In fact, the mean free path of nucleons with energies around the free NN \rightarrow NN π threshold (292 MeV) is of the same order of magnitude as the nuclear radii and any kind of processes between the above extreme cases can be responsible for the pion production.

The energy dependence of the experiments using the Ne beam between 125 and 400 MeV/nucleon and detecting low energy pions at forward angles has been roughly reproduced by the thermal fireball model³⁴). The isotropic angular distributions of the pions were in agreement with the predictions of such a model. The single nucleon model³⁵) calculations, in which a large $\sigma(0^\circ)/\sigma(90^\circ)$ ratio is predicted, agree with the absolute cross sections only at 125 MeV/nucleon.

The low-energy pion spectra measured at large angles with the ^{12}C beam at 86 MeV/nucleon²³) have been compared to a NN collision model calculation³⁶) based on the assumption that the interaction of the two nuclei is that of two diffuse nucleon momentum spheres, and taking into account Pauli blocking and pion absorption. Fig.5 shows the calculated invariant spectra and the experimental results. Harmonic oscillator momentum distributions

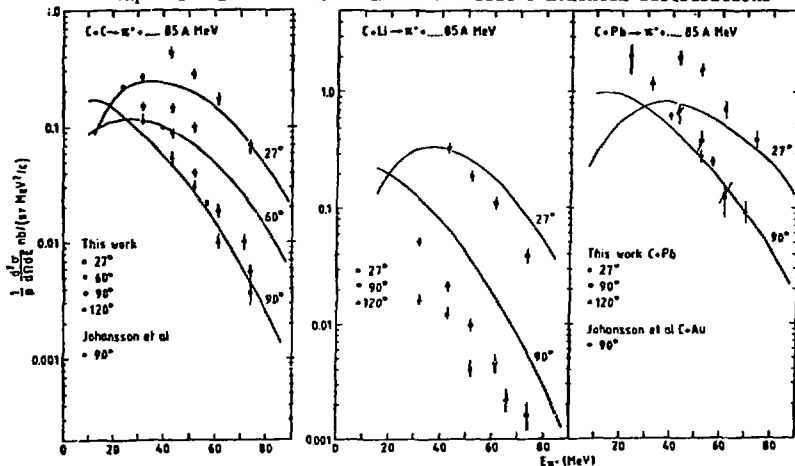


Fig.5. Comparison of the invariant $A(^{12}\text{C}, \pi^+X)$ cross sections with a single nucleon-nucleon model calculation.

have been assumed for ^7Li and ^{12}C and a Gaussian internal momentum distribution has been used for ^{208}Pb . The calculation reproduces the overall shape of several spectra but generally fails in the prediction of the angular distributions and the absolute cross sections. On the other hand, the angular distributions plotted in the NN center-of-mass and in the nucleus-

nucleus CM seem to point out in the $^{12}\text{C} + ^{197}\text{Au}$ case²²), that the production source has a velocity between the nucleus-nucleus and the nucleon-nucleon velocities and could correspond to the creation of a locally heated dense subvolume of nuclear matter.

The measurements of pion spectra up to the kinematic limit in the ($^3\text{He}, \pi X$) experiments²¹) and to a lesser extend in the ($^{12}\text{C}, \pi X$) experiment²⁴) could be compared to many different model predictions.

The simplified hard scattering model prediction for the invariant differential cross sections of the forward emitted pions is the well known $(1 - X_F)^n$ law³⁷), where X_F is the fractional longitudinal CM momentum of the pion and the exponent n depends on the number of constituents participating in the reaction. Such an expression fitted well the relativistic energy results at forward angles which scaled with energy and were independent of the target. At 303 MeV/nucleon the adjusted exponent values n are different for different targets and considerably smaller than the theoretical predictions²¹). One may conclude that scaling is no more present at lower energies where the forward emitted pions are no more uniquely due to the so called projectile fragmentation. The results obtained with deuterons at 300 and 600 MeV²⁵) confirm these conclusions.

An improved $NN \rightarrow NN\pi$ calculation describing π production in nucleus-nucleus collisions is the Constituent Interchange Model (CIM)³⁸). Here the two interacting nuclei undergo fragmentation into active and spectator constituents and the important ingredients are the structure functions of the two nuclei and the "elementary" production cross sections. In such a calculation,

the elementary cross sections are introduced semi-phenomenologically from the parametrization of the available $NN + \pi X$ data and the structure functions are obtained in the Infinite Momentum Frame, taking into account most of the physical assumptions i.e. high off-shell components and correct treatment of the fragmentation vertices. The calculation was performed for the ($^3\text{He}, \pi X$) reaction at 303 MeV/nucleon and the results were found to be in reasonable agreement with the data²¹) which extend over seven orders of magnitude (fig. 6). The CIM scheme appears to be the framework for a quantitative estimate of pion production in nucleus-nucleus collisions on the basis of the elementary process $NN + \pi X$, at least above 300 MeV/nucleon.

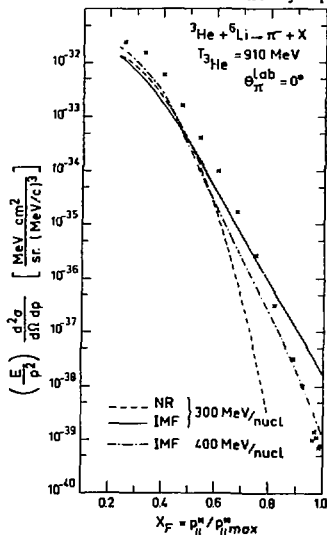


Fig.6. Comparison of the $^6\text{Li}(^3\text{He}, \pi X)$ invariant cross sections with the CIM calculation.

The quasi-two-body-scaling idea was originally made³⁹) for the analysis of different backward production experiments of energetic protons, K^- and antiprotons below threshold. The double differential cross sections scaled when plotted against k_{min} , the minimum internal momentum of nucleons in the target,

required to produce the observed particle, in a quasi-two-body interaction with the projectile. The same exponential behaviour was also observed for backward produced pions⁴⁰). The exponential function describing the data could be possibly related to an exponential internal momentum distribution of nucleons of the form $F(k) \sim 1/k \exp(-k/k_0)$, valid in the momentum range $0.4 < k < 1.5 \text{ GeV}/c$ ⁴¹).

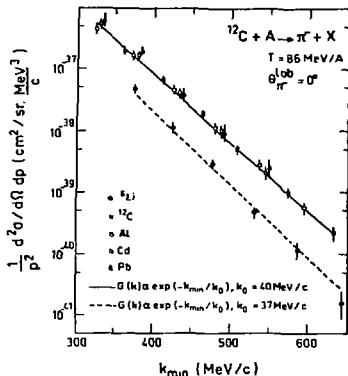


Fig.7. Quasi-Two-Body-Scaling of the ($^{12}\text{C}, \pi\text{-X}$) reaction data.

each containing M target- and N projectile-nucleons. Each contribution is given by the product of a formation cross section for each group $\sigma_{AB}(M, N)$ and of the probability distribution function $F_{MN, \pi}(p_{\pi})$ that M and N nucleons produce m pions with a momentum p_{π} . The pion production is described by Fermi's statistical model and the configuration phase space volume is a free parameter described by a density ρ_c , smaller than the normal nuclear density.

The theory reproduced the ($^3\text{He}, \pi\text{-X}$) data at 910 MeV with a rather low density parameter $\rho_c \approx 0.04 \text{ fm}^{-3}$ ²¹). In order to reproduce the ($^{12}\text{C}, \pi\text{-X}$) results²⁴) at 86 MeV/nucleon the above model was extended⁴⁴) to include the possibility of forming composite nuclei in the final channel. The average cluster size deduced from best fit to the data is between 2 and 3 (fig.8). Similar conclusions could be drawn from the comparison of the model with the large angle $^{12}\text{C}(\pi, \text{X})$ data²²).

A quite different picture has been proposed⁴⁵) for the coherent pion production based on the Weizsäcker-Williams method, wellknown in the theory of the electromagnetic field at high energies and already used in nuclear physics²⁸). The projectile nucleus is surrounded by a virtual pion cloud and this virtual pion field in the projectile CM represents a source of

In analogy to the backward production, pions at 0° should carry informations essentially on the projectile. When plotted as a function of k_{\min} , the data can be represented (fig.7) by an exponential function of the form $\exp(-k/k_0)$ with $k_0 \sim 40 \text{ MeV}/c$, slightly varying with the target mass^{21,24}). The latter variation confirms that at lower energies the forward observed particles may also carry information on the target. The spectra should then be described by the product of two similar structure functions, as opposed to the 180° produced spectra, where only the target structure function can be present.

An alternative way of producing pions is offered in the statistical model⁴²). Here, the observed particles have suffered a limited number of collisions within a well defined subgroup of active participants. The final momentum distribution corresponds to a random occupation of the accessible phase space. The pion cross section is an incoherent sum over the contributions arising from different groups of interacting tubes,

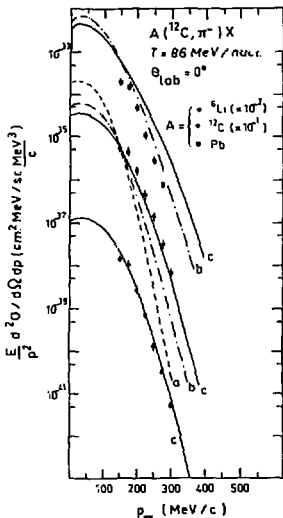


Fig.8. The extended statistical model calculation with cluster sizes of mass $a=1$, $b=2$ and $c=3$.

real pions in the laboratory, in analogy to the Coulomb field of a moving charge representing a photon source.

The effective pion number is given by the square of the pion field, deduced from the solution of the Klein-Gordon equation. The energy distribution of the pions is determined by the density distribution of the source and the observed pions result from the incoherent sum of πN interactions in the target, through which the pion momentum is reduced to its on-shell value.

In fig.9) the theoretical result⁴⁵⁾ is compared to the experiment. The exponential behaviour of the cross sections with ω^2 , the pion energy squared, is already reflected in the pion spectrum per energy, contained in the incoming ${}^3\text{He}$. The model is successful in reproducing the experimental pion spectrum over five orders of magnitude with the exception of the low energy region where many difficulties could be responsible for the overestimated cross sections (absorption, Δ width and position, etc.).

The presently available data do not allow to distinguish between the different reaction models proposed for the pion production. The measurement of the complete inclusive spectra produced at different energies around the free $NN \rightarrow NN\pi$ threshold, possibly at forward and backward angles, would put serious constraints on the theoretical models.

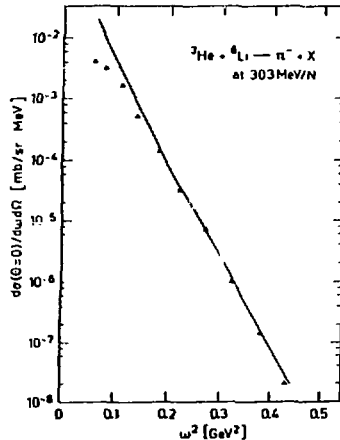


Fig.9. Comparison of the pionic cloud model predictions for the ${}^6\text{Li}({}^3\text{He}, \pi^- X)$ reaction with the experiment.

Doubly coherent pion production

The exclusive or doubly coherent pion production in nucleus-nucleus collisions is expected to have rather low cross sections as the result of the pion production itself and the weak superposition between initial and final states at high momentum transfers. In the (p, π) reaction, the high momentum transfers traduce themselves in high angular momentum mismatch between the initial and the final states which are enhanced. In nucleus-nucleus collisions such high momentum transfers can be shared between the participating nucleons or clusters in a variety of ways and one would expect less sensitivity to the angular momentum mismatch between initial and final nuclear states, as well as a preferential production of collective nuclear states.

The experimental search for doubly coherent pion production implies the use of high resolution magnetic spectrometers $\Delta E \sim 1$ MeV and the availability of high intensity ion beams ($>10^{11}$ pps). These requirements explain the rather limited number of experiments and the scarcity of good quality experimental data.

The $({}^3\text{He}, \pi^-)$ reaction

First evidence of doubly coherent pion production was found at CERN²¹⁾ with the intense, a few 10^{12} pps, and high duty cycle ${}^3\text{He}$ beam of 910 MeV.

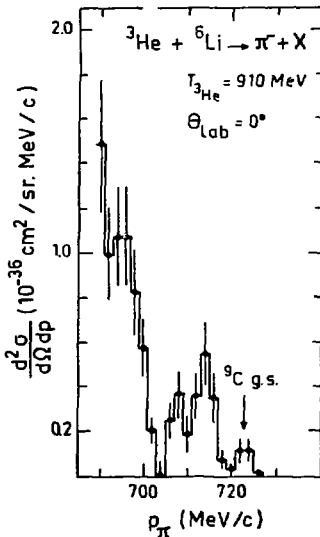


Fig.10. Single pion spectrum of the reaction ${}^3\text{He} + {}^6\text{Li} \rightarrow \pi^- + X$. Discrete pion groups to the ${}^9\text{C}$ g.s. and to states around 9 and 15 MeV excitation are observed.

The doubly coherent reaction ${}^3\text{He} + {}^6\text{Li} + \pi^- + {}^9\text{C}$ was found to have a differential cross section of ~ 10 pb/sr, integrated over ~ 25 MeV excitation in the residual nucleus. A first indication of the strong target mass dependence of the production cross section was given by the ${}^3\text{He} + {}^9\text{Be} + \pi^- + {}^{12}\text{N}$ reaction for which the cross section would be ≤ 1.5 pb/sr. Recently⁴⁶⁾ an improved experiment, using the OMICRON spectrometer for high resolution momentum analysis of the produced pions, confirmed the first result with an integrated differential cross section of 4.2 ± 0.6 pb/sr. With a resolution of 3.2 MeV (FWHM) at $T_\pi = 623.3$ MeV, pions to the ${}^9\text{C}$ g.s. and the 2.2 MeV state couldn't be resolved and the corresponding cross section is 0.58 ± 0.23 pb/sr. A rather strong pion transition leading to an excitation energy around 9 MeV in ${}^9\text{C}$ was observed with a cross section of 2.3 ± 0.5 pb/sr (fig.10) No states have been reported so far at high excitations in ${}^9\text{C}$ the above state could be the isobaric analogue of collective states in ${}^9\text{Be}$, like the suggested resonance at ~ 23 MeV⁴⁷⁾.

The (d, π^-) reaction

The variable energy intense deuteron beam at Saturne was used to study the (d, π^-) reaction at 300 and 600 MeV. The high resolution magnetic spectrometer SPES I was used for the pion detection. Discrete pion groups from the $d + {}^6\text{Li} \rightarrow \pi^- + {}^8\text{B}$ reaction could be observed²⁵⁾ leading to the ${}^8\text{B}$ g.s. (2^+), 0.78 MeV (?) and to the 2.32 MeV (3^+) states (table 1). The momentum transfer, 4.6fm^{-1} at 300 MeV and 5.8fm^{-1} at 600 MeV dominates the cross sections, which are higher at the lower incident energy, far below the free $\text{NN} \rightarrow \text{NN}\pi$ threshold.

Table 1 : Differential cross sections for the ${}^6\text{Li}(d,\pi^-){}^8\text{B}$ reaction in pb/sr

T_d	${}^8\text{B}$ g.s. (2^+)	${}^8\text{B}$ 0.78 MeV ()	${}^8\text{B}$ 2.32 MeV (3^+)
300	520 ± 120 (740) ⁵⁷⁾	710 ± 140	1330 ± 160 (1650) ⁵⁷⁾
600	75 ± 30 (50) ⁵⁷⁾	85 ± 30	240 ± 40 (170) ⁵⁷⁾

The trend of the cross section to increase at lower energies was consistent with the cross section measured for the inverse reaction⁴⁸⁾ ${}^{12}\text{C}(\pi^+,d)$ at $T_\pi = 49.3$ MeV, which is equivalent to the (d, π) reaction at 195 MeV with a momentum transfer of 3.3fm^{-1} and a differential cross section of 3000pb/sr . DWBA calculations of the ${}^{12}\text{C}(\pi^+,d){}^{10}\text{C}$ reaction⁴⁹⁾ yield the right order of magnitude for the cross sections. For the (d, π) reaction a DWBA prediction exists only at 185 MeV⁵⁰⁾.

The (${}^3\text{He},\pi^+$) reaction

Most of the recent data on double coherent production have been obtained in studying this reaction.

The measurements at lower energies have been performed using the high intensity (several μA) and variable energy ${}^3\text{He}$ beam of the Orsay synchrotron. A 180° magnetic spectrometer is used for the pion detection with resolutions of the order of 2 MeV. Many experiments have been performed on several light targets (${}^3\text{He}$ ⁵¹⁾, ${}^4\text{He}$ ⁵²⁾, ${}^6\text{Li}$, ${}^{10}\text{B}$ ⁵³⁾) at incident energies between 235 and 283 MeV and all of them were successful in observing the corresponding doubly coherent reaction (${}^3\text{He},\pi^+$). Very recently, the energy dependence of the ${}^3\text{He} + {}^3\text{He} \rightarrow \pi^+ + {}^6\text{Li}$ reaction has been studied between 350 and 600 MeV⁵⁴⁾ using the variable energy beam of the Saturne Synchrotron. The high resolution spectrometer SPES I was used for these experiments with an energy resolution of ≤ 1 MeV.

The ${}^3\text{He} + {}^3\text{He} \rightarrow \pi^+ + {}^6\text{Li}$ reaction studied at 268.5 MeV and at 282 MeV has considerable cross sections (a few tens of nb/sr) for transitions to the ${}^6\text{Li}$ g.s. (1^+) 2.18 MeV (3^+) and 3.56 MeV (0^+) states⁵¹⁾. The low pion energy made possible the comparison of the ${}^6\text{Li}$ g.s. results to those obtained from pionic atoms. The ${}^3\text{He} + {}^3\text{He} \rightarrow \pi^+ + {}^6\text{Li}$ amplitude can indeed be related to the imaginary part of the $\pi{}^6\text{Li} \rightarrow \pi{}^6\text{Li}$ amplitude, estimated from

pionic atom shifts and widths through the pion absorption cross section and the optical theorem. The value of the squared transition amplitude $\langle |f^2| \rangle_{k_{\pi=0}} = (7.8 \pm 2.2) \cdot 10^{-6} \text{fm}^2$ derived from the pionic atom data⁷⁾ and corresponding to a ${}^3\text{He}$ energy of 251 MeV, is in agreement with the values $(7.6 \pm 0.7) \cdot 10^{-6} \text{fm}^2$ and $(8.3 \pm 0.5) \cdot 10^{-6} \text{fm}^2$ deduced from the pion production experiment⁵¹⁾.

The ${}^3\text{He} + {}^4\text{He}$ reaction was studied at 266.5 and at 280.5 MeV. Transitions to the ${}^7\text{Li}$ g.s. ($3/2^+$) and 0.478 MeV ($1/2^-$) (unresolved) and to the 4.63 MeV ($7/2^-$) states could be observed with cross sections comparable to those obtained with the ${}^3\text{He}$ target. The $7/2^-$ state of ${}^7\text{Li}$ is not preferentially excited in the $({}^3\text{He}, \pi^+)$ reaction, as it was the case in the ${}^6\text{Li}$ (p, π^+) ${}^7\text{Li}$ reaction, where this higher orbital momentum state was favoured⁵⁵⁾

The ${}^3\text{He} + {}^6\text{Li} + \pi^+ + {}^9\text{Be}$ and the ${}^3\text{He} + {}^{10}\text{B} + \pi^+ + {}^{13}\text{C}$ reactions (fig. 11) take place with differential cross sections of the same order of magnitude⁵³⁾, a few tens of pb/sr, but considerably smaller than those measured for the light targets. Unlike the low energy (p, π^+) data on heavier targets, the ${}^3\text{He} + {}^6\text{Li} + {}^9\text{Be} + \pi^+$ have the same smooth decrease with angle as many (p, π) reaction far from the production threshold.

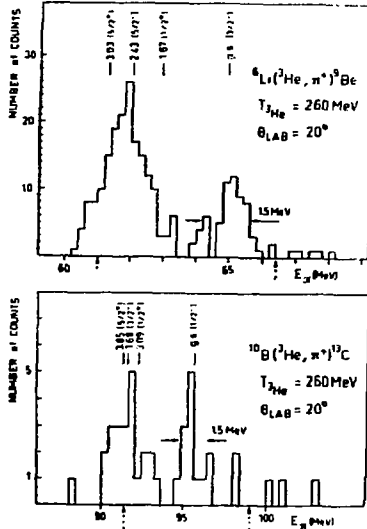


Fig. 11.

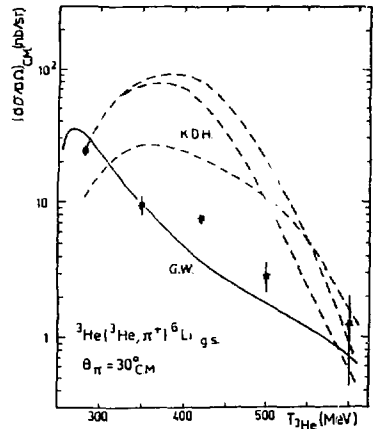


Fig. 12. Pionic fusion model (K.D.H.) and semi-phenomenological model (G.W.) predictions and measured excitation function of the ${}^3\text{He}({}^3\text{He}, \pi^+){}^6\text{Li}$ g.s. reaction

The recent study of the ${}^3\text{He} + {}^3\text{He} \rightarrow \pi^+ + {}^6\text{Li}$ reaction measured the production cross section for transitions to the ${}^6\text{Li}$ g.s. (1^+) and 2.18 MeV (3^+) state at 350, 420, 500 and 600 MeV and at laboratory angles of 15° and 40° . Fig. 12) shows the energy dependence of the $(15^\circ_{\text{LAB}}) 30^\circ_{\text{CM}}$ cross section corresponding to the ${}^6\text{Li}$ g.s., in which the Orsay data at 283 MeV was included⁵¹⁾ The decrease of the production cross section with the incident energy already noticed at lower energies is confirmed over an energy scale of 300 MeV.

Table 2 summarizes the observed production cross sections, integrated over all observed final states for the different doubly coherent reactions, studied generally at forward angles.

Table 2 : Doubly coherent π production cross sections (nb/sr)

beam	target	T_{in} (MeV/nuclei)	90	117	140	150	167	200	300
d	${}^6\text{Li}$					2.5 (4.6fm^{-1})			0.4 (5.8fm^{-1})
${}^3\text{He}$	${}^3\text{He}$		180	71	45		31	18	
	${}^4\text{He}$		190						
	${}^6\text{Li}$		0.28						0.006 (8.5fm^{-1})
	${}^9\text{Be}$								≤ 0.0015
	${}^{10}\text{B}$		0.16						

The conclusions from these first experiments are the following :

- for a given reaction the cross sections decrease with incident energy (one order of magnitude from 90 to 200 MeV/nucleon in the ${}^3\text{He} + {}^3\text{He}$ reaction and 2 orders of magnitude in the ${}^3\text{He} + {}^6\text{Li}$ reaction)
- for a given projectile the cross sections decrease rapidly with the target mass (ex. three orders of magnitude going from ${}^3\text{He}$ to ${}^{10}\text{B}$ targets at 90 MeV/nucleon)
- for a given target the cross sections decrease rapidly with the projectile mass (about two orders of magnitude between d + ${}^6\text{Li}$ and ${}^3\text{He} + {}^6\text{Li}$ at 300 MeV/nucleon)
- the production cross sections depend apparently very strongly on the momentum transfer and less on the available C.M. energy.

The comparison to theoretical models of the coherent pion production

Two different models have been proposed for the description of the doubly coherent pion production.

The pionic fusion model was first proposed in 1978, and in its final formulation it was used to predict the differential cross sections for the ${}^3\text{He} + {}^3\text{He} \rightarrow \pi^+ + {}^6\text{Li}$ reaction^{29,56}) and the reaction (d, π^-)⁵⁷). In this model (fig.13) pions exchanged between two interacting nucleons in the projectile and in the target nuclei lead to a $\Delta(3,3)$ excitation which serves as energy reservoir, propagates in the nuclear matter produced by the two fused nuclei and finally decays through pion emission. The suggested mechanism is quite plausible and economical with regard to the momentum transfer shared between the two nuclei. The model prediction⁵⁷) for the differential cross section of the d + ${}^6\text{Li} \rightarrow \pi^- + {}^8\text{B}$ reaction are in good agreement with the experimental data at 300 and at 600 MeV²⁵) (see Table 1). For the energy dependence of the ${}^3\text{He} + {}^3\text{He} \rightarrow \pi^+ + {}^6\text{Li}$ reaction the model predicts a smooth increase for the cross section from threshold to ~ 400 MeV and then a decrease by a factor of ~ 100 at 600 MeV.

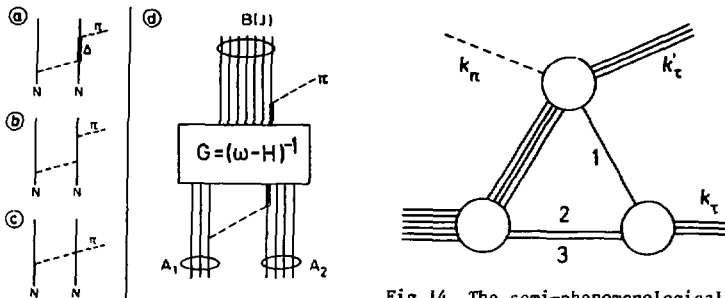


Fig.13. The pionic fusion model

An alternative semi-phenomenological theoretical approach⁵⁸⁾ describes the $({}^3\text{He}, \pi)$ reaction in terms of the ${}^3\text{He} + p \rightarrow \pi^+ + {}^4\text{He}$ "elementary" reaction on individual protons of the target. The recoiling ${}^4\text{He}$ is then captured by the spectator nucleons to form the final nucleus. In the case of the ${}^3\text{He} + {}^3\text{He} \rightarrow \pi^+ + {}^6\text{Li}$ reaction the relationship to the above "elementary" reaction is established through the inverse reaction $\pi^+ + {}^6\text{Li} \rightarrow {}^3\text{He} + {}^3\text{He}$ and the relation between the amplitudes $f_{\pi}({}^6\text{Li} \rightarrow {}^3\text{He} + {}^3\text{He})$ and $f_{\pi}({}^4\text{He} \rightarrow p + {}^3\text{He})$ (fig.14). Since ${}^6\text{Li}$ is reasonably well described in terms of a cluster-model as an alpha particle coupled to a deuteron or a quasi-deuteron, the model requires that after the pion absorption on the alpha particle, the final state interaction between the emitted proton and the spectator nucleons (quasideuteron or deuterons) leads to the ${}^3\text{He}$.

Fig.14. The semi-phenomenological description of the ${}^3\text{He} + {}^3\text{He} \leftrightarrow \pi^+ + {}^6\text{Li}$ reactions.

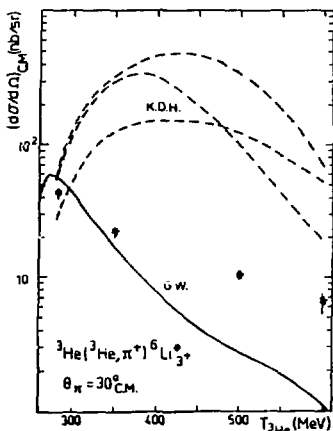


Fig.15. Pionic fusion (K.D.H.) and semi-phenomenological model (G.W.) predictions and measured excitation function of the ${}^3\text{He}({}^3\text{He}, \pi^+){}^6\text{Li}^*(3^+)$ reaction.

The experimental inputs to the model are the cross sections of the three nucleon transfer reaction ${}^3\text{He} + p \rightarrow \pi^+ + {}^4\text{He}$ for which small angle data are needed. The calculations⁵⁹⁾ shown below were performed using the recent ${}^3\text{He} + p \rightarrow \pi^+ + {}^4\text{He}$ results⁸⁾ at 600 MeV between 5° and 30°_{LAB} , corresponding to the angular range of 170° to 120°_{CM} for the $p + {}^3\text{He}$ reaction at 200 MeV (see fig.1). The energy dependence predicted by this model is a monotonic exponential decrease between 300 and 600 MeV.

The experimental data for the ${}^6\text{Li}$ g.s. (fig.12) would favour the semi-phenomenological model compared to the pionic fusion model. As we can see (fig.15) the situation is worse for the ${}^6\text{Li}(3^+)$ 2.18 MeV level. The monotonic decrease of the data is considerably weaker than predicted by the semi-phenomenological model. The energy dependence of the pionic fusion model is not observed experimentally, specifically no maximum around 400 MeV is found for either transition to ${}^6\text{Li}$.

Although the adequate choice of nuclear wave functions could improve the theoretical calculation and the introduction of distortion and of the final state interactions would improve the semi-phenomenological calculation, it is difficult to imagine how the shape of the energy prediction in the two models could be changed. The pionic fusion model gave reasonable values of the ${}^6\text{Li}(d,\pi)$ reaction cross sections at two different energies but fails in reproducing the energy dependence of the ${}^3\text{He} + {}^3\text{He} \rightarrow \pi^+ + {}^6\text{Li}$ reaction. The semi-phenomenological model gave reasonable results on several (${}^3\text{He},\pi^+$) reactions at lower energies and reproduced semi-qualitatively the angular distributions and the energy dependence at lower energies.

The doubly coherent π production is far from being understood but one should remember that the first experiments in the field only started in 1978 at CERN. The availability of high intensity beams will improve the quality of the experiments, which in the very near future will be possible only with light projectile-target combinations. A smaller number of experiments, covering a large angular and incident energy range would be preferable in order to put the necessary constraints on the development of predictive theoretical models.

REFERENCES

- 1) J.J. Domingo et al., Phys. Lett. 32B, 309 (1970); S. Dahlgren et al. Phys. Lett. 35B, 219 (1971); see also the review article by H.W. Fearing, Progr. Part. Nucl. Phys. 7, 113 (1981) and refs therein.
- 2) J. Le Tourneux and J. Eisenberg, Nucl. Phys. 87, 331 (1966).
- 3) A. Reitan, Nucl. Phys. B29, 525 (1971); B50, 166 (1972).
- 4) N. Willis et al., J. Phys. G. NP7, 195 (1981).
- 5) L. Bimbot and Y. Le Bornec, private communication.
- 6) B. Höistad et al., Phys. Lett. 79B, 385 (1978)

- 7) J. Hüfner, L. Tauscher, C. Wilkin, Nucl. Phys. A231, 454 (1974).
- 8) Orsay-Strasbourg-Saclay collaboration, to be published.
- 9) F. Soga et al., Phys. Rev. C22, 1348 (1980).
- 10) F. Soga et al., Phys. Rev. C24, 570 (1981).
- 11) S. Dahlgren et al. Nucl. Phys. A227, 245 (1974).
- 12) R.E. Anderson et al., Phys. Rev. C23, 2616 (1981).
- 13) G.J. Lolos et al. Phys. Rev. C, to be published
- 14) T.P. Sjoreen et al., Phys. Rev., C24, 1135 (1981).
- 15) B. Höistad, IUCF Bloomington, AIPCP 79, 389 (1982) and to be published.
- 16) P. Berthet et al. Phys. Lett. 106B, 465 (1981).
- 17) C.W. Barry, Phys. Rev. D7, 1441 (1973).
- 18) R. Frascaria et al., Int. Conf. Nucl. Phys., Florence 1983.
- 19) R. Frascaria, private communication.
- 20) B. Mayer et al., to be published.
- 21) E. Aslanides et al., Phys. Rev. Lett. 43, 1466 (1979); Phys. Rev. Lett. 45, 1738 (1980). E. Aslanides et al. Nucl. Phys. A393, 314 (1983).
- 22) T. Johansson et al., Phys. Rev. Lett. 48, 732 (1982).
- 23) V. Bernard et al., Nucl. Phys., to be published.
- 24) E. Chiavassa et al., to be published.
- 25) E. Aslanides et al., Phys. Lett. 108B, 91 (1982).
- 26) W. Benenson et al., Phys. Rev. Lett. 43, 683 (1979).
- 27) S. Nagamiya et al., Phys. Rev. Lett. 48, 1780 (1982).
- 28) G.E. Brown and P.A. Deutschmann, Proc. Workshop on High Resolution Heavy Ion Phys., Saclay 1978.
- 29) K. Klingenberg, M. Dillig, M. G. Huber, Phys. Rev. Lett. 47, 1654 (1981).
- 30) S.J. Lindenbaum and R.M. Sternheiner, Phys. Rev. 105, 1874 (1957).
- 31) J.P. Sullivan et al. Phys. Rev. C25, 1499 (1982).
- 32) M. Gyulassy and S.K. Kauffmann, Nucl. Phys. A362, 503 (1981).
- 33) E. Aslanides et al. Nuovo Cim. Lett. 34, 385 (1982).
- 34) J.I. Kapusta, Phys. Rev. C16, 1494 (1977).
- 35) G. Bertsch, Phys. Rev. C15, 713 (1977).
- 36) J.P. Bondorf et al., Univ. of _____, preprint LUIP 8302, 1983.
- 37) I.A. Schmidt and R. Blankenbecler, Phys. Rev. D15, 3321 (1977).
- 38) M. Chemtob, Nucl. Phys. A14, 387 (1979) and private communication.
- 39) R.D. Amado and R.M. Woloshyn, Phys. Rev. Lett. 36, 1435 (1976).
- 40) C.F. Perdrisat, S. Frankel and W. Frati, Phys. Rev. C18, 1764 (1978).
- 41) R.D. Amado and R.M. Woloshyn, Phys. Lett. 62B, 253 (1976).
- 42) J. Knoll, Phys. Rev. C20, 773 (1980); Nucl. Phys. A343, 511 (1980).
- 43) S. Bohrmann and J. Knoll, Nucl. Phys. A356, 498 (1981).
- 44) R. Shyam and J. Knoll, GSI preprint 83-22 and private communication.
- 45) B. Hiller and H.J. Pirner, Phys. Lett. 109B, 338 (1983)
- 46) T. Bressani et al. to be published.
- 47) F. Ajzenberg-Selove, Nucl. Phys. A320, 1 (1979).
- 48) J.F. Amann et al. Phys. Rev. Lett. 40, 758 (1978).
- 49) M. Betz and A.K. Kerman, Nucl. Phys. A345, 493 (1980).
- 50) M. Dillig et al., Lett. Nuovo Cim. 18, 487 (1977).
- 51) Y. Le Bornec et al., Phys. Rev. Lett. 47, 1870 (1981).
- 52) L. Bimbot et al., Phys. Lett. 114B, 311 (1982).
- 53) N. Willis et al., Phys. Lett. B, to be published.
- 54) Y. Le Bornec et al., Phys. Lett. 133B, 149 (1983).
- 55) T. Bauer et al., Phys. Lett. 69B, 433 (1977).
- 56) M.G. Huber and K. Klingenberg, IUCF Bloomington, AIPCP 79, 389 (1982).
- 57) M. Dillig, note CEA N2276, p. 113 (1981).
- 58) J.F. Germond and C. Wilkin, Phys. Lett. 106B, 449 (1981).
- 59) J.F. Germond and C. Wilkin, private communication.

**Imprimé
au Centre de
Recherches Nucléaires
Strasbourg
1984**